Journal of Thermal Analysis, Vol. 49 (1997) 1025-1037

TEMPERATURE RESOLVED X-RAY DIFFRACTION AS A TOOL OF THERMAL ANALYSIS

W. Engel, N. Eisenreich, M. Herrmann and V. Kolarik

Fraunhoferinstitut für Chemische Technologie, D-76327 Pfinztal-Berghausen, Germany

Abstract

Time and temperature resolved X-ray diffraction was used for thermal analysis. Series of diffraction patterns were measured, while the samples are heated/cooled stepwise or isothermally with freely selectable temperature programs.

The method was applied for the investigation of the phase transitions of ammonium nitrate and HMX (1,3,5,7-tetranitro-1,3,5,7-tetraaza-cyclooctane), when the identification of phases was required. Its capability in the field of kinetics is demonstrated with the isothermal investigation of the solid state reaction of ammonium nitrate with copper oxide and the non-isothermal investigation of the high temperature corrosion of nickel, which was performed by means of a difference procedure. For obtaining structural details peak fitting and Rietveld refinement were applied for the investigation of ammonium nitrate and HMX.

Keywords: crystallographic evaluation, evaluation with difference procedure, kinetics, Rietveld refinement, X-ray diffraction, temperature resolved

Introduction

In thermal analysis the properties of materials are monitored as a function of temperature with a linear function of time. The classical procedures as DSC and TG are increasingly complemented by techniques which yield more detailed information like time and temperature resolved X-ray diffraction. This method is especially suited, when unambiguous results are required about solid state reactions and phase transitions involving crystalline materials. The series of diffraction patterns that are measured, while the samples are heated continuously, stepwise or isothermally, contain all informations about occurring phases, their concentration, their structural details and their changes during the selected temperature program.

While single X-ray diffraction patterns at non-ambient temperatures were already measured in the earlier days of X-ray diffraction, the measurement of series of hundreds of patterns, which are necessary for a real thermal analysis by means of X-ray diffraction, became possible after the development of fast semiconductor detectors at the end of the sixties [1] and of position sensitive proportional counters in the seventies [2]. The availability of more intensive X-ray sources as rotating anodes or synchroton radiation has contributed to this development in the same way as the automated measurements accessible by the progress of the computer techniques.

0368–4466/97/ $ 5.00

John Wiley & Sons Limited
Chichester

The application of the new technique is reported for examples, where the identification of phases, the kinetics of solid state reactions, structural informations as a function of time and temperature are required that cannot be provided by the classical procedures as DSC and TG. The examples include phase transitions of ammonium nitrate (AN) and HMX (1,3,5,7-tetranitro-1,3,5,7-tetraaza-cyclooctane), where the identification of the phases is required. The determination of the solid state kinetics from isothermal and non-isothermal measurements is reported for the reaction of ammonium nitrate with copper oxide and the high temperature corrosion of nickel, and the extraction of structural details is described for the phases of ammonium nitrate.

Measurements

The measurements were performed with a system described elsewhere [3]. It consists of an X-ray diffractometer Siemens D5000 combined with a low temperature device of Paar and high temperature devices HTK 10 of Paar and HDK 2.4 of Bühler. With a fast position sensitive proportional counter of Braun series of more than 200 angle dispersive diffraction patterns per day can be measured, while the samples are heated and cooled linearly or stepwise with freely selectable temperature programs. In this way the samples can be monitored *vs.* temperature or time. The different series were measured with the following parameters:

Structural details of AN

copper and chromium radiation, position sensitive proportional counter
angular range 10–100°C, measured with 12°C min^{-1}
temp. range –70–150°C, stepwise heating with temp. intervals of 3°C,
during transitions 0.25°C

Phase transitions of HMX

chromium radiation, position sensitive proportional counter
angular range: 25–65°C, measured with 30°C min^{-1}
temp. range –100–240°C, stepwise heating with temp. intervals of 10°C,
during transitions of 1°C

Reactions of AN with CuO, molar ratios 2:1, 4:1, 8:1

chromium radiation, position sensitive proportional counter
angular range: 25–65°C, measured with 30°C min^{-1}
continuous isothermal measurements at 100, 105, 110, 115, 120°C
after heating with 60°C min^{-1}

High temperature corrosion of nickel

copper radiation, scintillation counter
angular range 36–77°C, measured with 10°C min^{-1}
temp. range 10–1000°C, stepwise heating with temp. intervals of 15°C
average heating rate 3°C min^{-1}

Evaluation

The identification of phases measured during heating/cooling cycles was performed by comparison with the PDF file of ICDD or by comparing with known patterns measured with pure substances under defined temperatures.

The kinetic evaluation was carried out by means of a difference procedure described elsewhere [4], which delivers the relative changes in the measured patterns during the reaction. The measured patterns are subtracted from the first pattern already measured. The sum $Y(t_j)$ of the absolute differences between the corresponding channel contents represents the changes in the diffraction patterns.

$$Y(t_j) = \sum_{i=1}^{n} \left| Y_i(t_1) - Y_i(t_j) \right|$$

j=number of the current diagram; i=number of the current channel; n=total number of channels, the channels representing angular values in angle dispersive measurements; t=time (temperature for non-isothermal runs). The procedure can be applied to the whole pattern or to selected angular ranges with specific diffraction peaks. The plots of the difference curves normalized to unity representing the progress of the reaction with time were used for kinetic analysis. The rate constants were computed by fitting the difference curves with the most suited kinetic model.

The structural information was obtained in 2 ways by peak fitting and whole pattern fitting. For peak fitting the position, peak intensity and peak width were determined by a least squares fit with a Lorentz function using programs developed in our group. The cell constants were fitted using the d-spacings computed from the peak positions. The peak positions, peak intensities, d (hkl) values, lattice constants and the volume of the unit cell were plotted as a function of time or temperature.

For whole pattern fitting developed by Rietveld for neutron diffraction [5] and adapted to X-ray diffraction by Young [6] a diffraction pattern is calculated based on the atom positions of an at least approximately known structure, given peakprofiles, underground and instrument functions. By varying the atom positions and other parameters the calculated is fitted to the measured pattern.

Application of the method

Identification of phases

Ammonium nitrate (AN) crystallizes in 5 phases. The structurally related phases I, II, IV and V appear on cooling dry AN from the melt after passing order/disorder transitions. The structurally not related phase III appears only in the presence of water, which helps to nucleate the phase [7, 8].

The existence of several phases in a narrow temperature range together with the complications caused by the presence of water makes it difficult to get unambiguous results with DSC and DTA, as these methods report thermal effects without identifying the occurring phases [14–18]. Therefore series of diffraction patterns were

Table 1 Phases of ammonium nitrate [9–13]

Phases	V	IV	III	II	I
Crystal system	orthorombic	orthorombic	orthorombic	tetragonal	cubic
Stability humid	<–18	–18/+32	32/84	84/125	125/melt
(°C) dry	<–18	–18/+55		55/125	125/melt

measured for determining the transition paths [19]. Figure 1 presents selected patterns of such a series.

With the temperature program 20/150/–70/150°C the transition sequence

$$IV \xrightarrow{55} II \xrightarrow{130} I \xrightarrow{119} II \xrightarrow{45} IV \xrightarrow{-40} V \xrightarrow{0} IV \xrightarrow{55} II \xrightarrow{125°C} I$$

was observed with dry AN confirming literature. With the program 20/100/–70/100°C, however, unexpected results were obtained showing the transitions

$$IV \xrightarrow{55} II \xrightarrow{47} V \xrightarrow{42–46} V+IV \xrightarrow{-40} V \xrightarrow{0} V+IV \xrightarrow{47}$$
$$II+IV \xrightarrow{55°C} II.$$

The hitherto unknown sequence means that on cooling phase II changes into V at about 47°C followed by a partial transition into IV. The complete transition into phase V occurs below –40°C. On reheating a part of the sample changes into phase IV at about 0°C. Phase V in the resulting mixture V/IV changes into II at 47°C, whereas the part of phase IV shows the known transition into phase II at 55°C. The measurements are reproducible, only the ratio of the coexisting phases IV/V shows some change in different measurements [19].

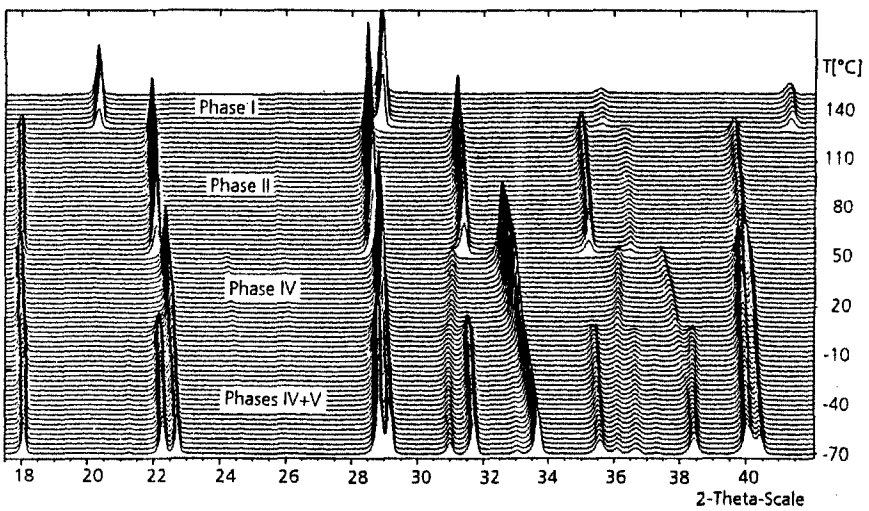

Fig. 1 Selected diffraction patterns of a series measured with ammonium nitrate

Kinetics from isothermal experiments

For demonstrating the determination of kinetic parameters from isothermal experiments measurements are presented with mixtures of ammonium nitrate with copper oxide [20], which react on heating to form diammine copper dinitrate:

$$2NH_4NO_3 + CuO \rightarrow [Cu(NH_3)_2](NO_3)_2 + H_2O$$

Selected patterns of a series measured at 120°C are shown in Fig. 2. The series acquired at 100, 105, 110, 115 and 120°C with a molar ratio of 4:1 were evaluated using the difference method described earlier. The rate constants were obtained by fitting the difference curves of the product peaks at different temperatures by a rate equation of type [21, 22]

$$y = 1-\exp[-K(T)t^n],$$

where y is the extent of transformation at given time t, and k is a temperature dependent rate constant independent of time. The experimental and the fitted curves of the product peaks at different temperatures are shown in Fig. 3.

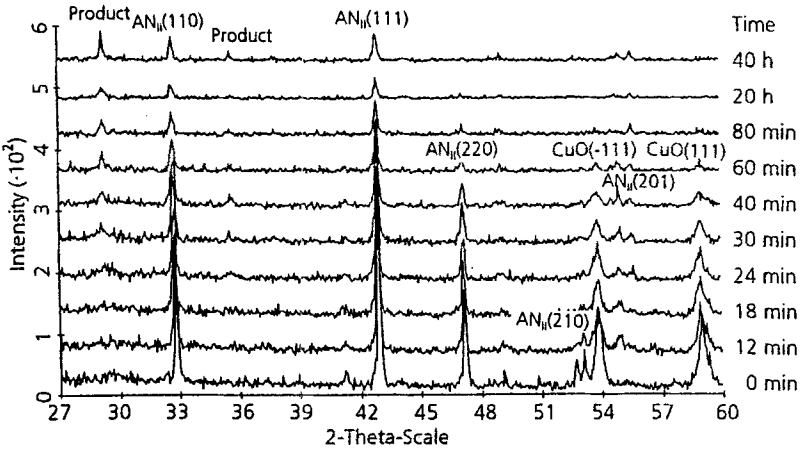

Fig. 2 Selected diffraction patterns of an isothermal series measured with a mixture of ammonium nitrate and copper oxide at 120°C, molar ratio 4:1

The experimental kinetic profiles were also analyzed using other mechanistic models, especially the Jander diffusion model for powdered reactants [22]. However, this model gives no good fit of the experimental profile especially at the initial stage of the reaction.

The observed behaviour in kinetic profiles is commonly associated with the nucleation and growth type of solid-state transformations. According to this mechanism, the reaction rate is controlled by the formation and growth of nuclei on the surface of the reactant. The value of n depends on the shape of the nuclei, the number of nuclei present at the beginning of the reaction and their distribution in the particles.

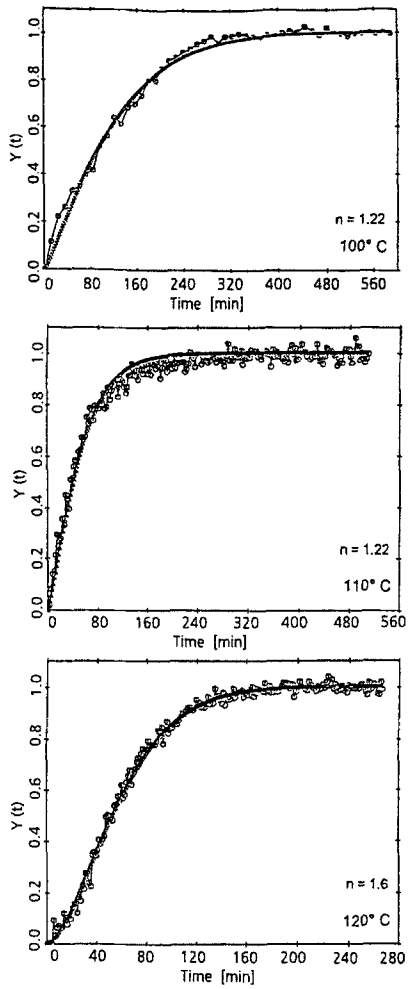

Fig. 3 Difference and fitted curves of the product peaks, calculated from isothermal series measured at 100, 110 and 120°C with a mixture of ammonium nitrate and copper oxide, molar ratio 4:1

An activation energy $E_a = 101.9$ kJ mol^{-1} and a frequency factor $z = 5.57 \cdot 10^{11}$ min^{-1}, see the Arrhenius plot Fig. 4, were calculated with the reaction constants at 100–115°C. The value at 120°C was not included, because it deviates from the tendency observed with the other constants, which may be due to the close neighbourhood of the phase transition II/I.

The observed rate of the solid state reaction between ammonium nitrate and copper oxide is slow for a 2:1 molar ratio increasing with an excess of ammonium nitrate i.e. a ratio of 4:1 and 8:1. The excess of ammonium nitrate increases the probability of copper oxide to find close contact with the nitrate surface.

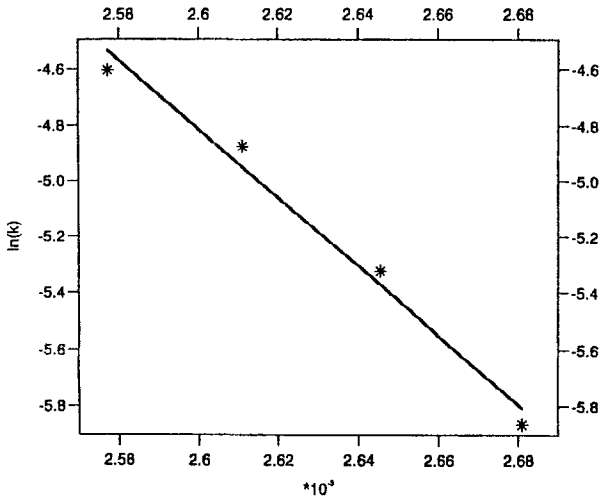

Fig. 4 Arrhenius plot of the reaction of ammonium nitrate with copper oxide, molar ratio 4:1

Kinetics from non-isothermal experiments

An example for using non-isothermal experiments is presented in the field of high temperature corrosion, where the formation of NiO is followed on a nickel surface [24]. The NiO-peaks of the measured series, see Fig. 5, were evaluated us-

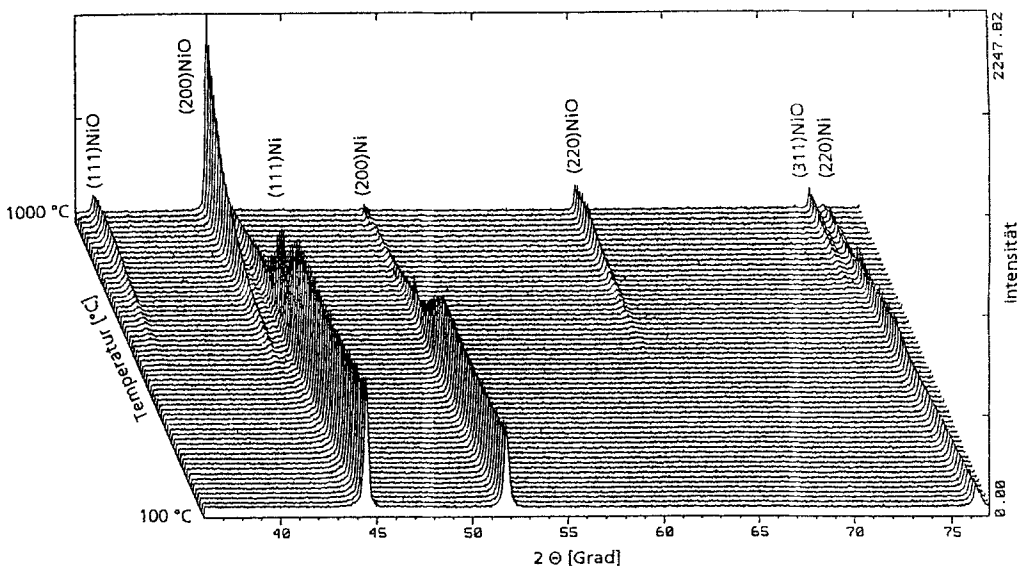

Fig. 5 Diffraction patterns of a non-isothermal series showing the high temperature corrosion of nickel

ing the difference procedure and fitted with a suited equation developed with the following consideration:

With	$x\mathrm{d}x=k\mathrm{d}t$	for parabolic growth
and	$\alpha=\mathrm{d}T/\mathrm{d}t$	for the heating rate
and	$k=z\exp(-E/RT)$	for the Arrhenius equation
after integration	$x(T)=\sqrt{2z/\alpha\int\exp(-E/RT)\mathrm{d}T}$	

is obtained for the thickness of the oxide layer as a function of temperature.

The observed intensities of the NiO reflections depend from the absorption of the X-rays on their way through the layer x with an absorption coefficient μ:

Lambert-Beer's law	$I=I_0\exp(-\mu s)$	for the intensity
inserting	$s=2x/\sin\alpha$	for the way through the layer
integrating 0 to x	$I=I_0\sin\alpha/2\mu[1-\exp(-2\mu/\sin\alpha\, x)]$	for the intensity originated by the layer.

Taking into account the conditions of X-ray diffraction with the structural parameters governing the intensity as well as the difference formation a proportionality factor f_c has to be included, before the equation for fitting the difference curve is obtained:

$$Y(T) = f_c \sin\alpha/(2\mu)[1-\exp(-2\mu/\sin\alpha x)$$

with

$$x(T) = \sqrt{2z/\alpha\int\exp(-E/RT)\mathrm{d}t}$$

described above for diffusion controlled, parabolic growth. The plot of a curve following the developed equation is plotted in Fig. 6 showing the growing oxide scale until the radiation can no longer penetrate the whole layer with the curve reaching a constant value.

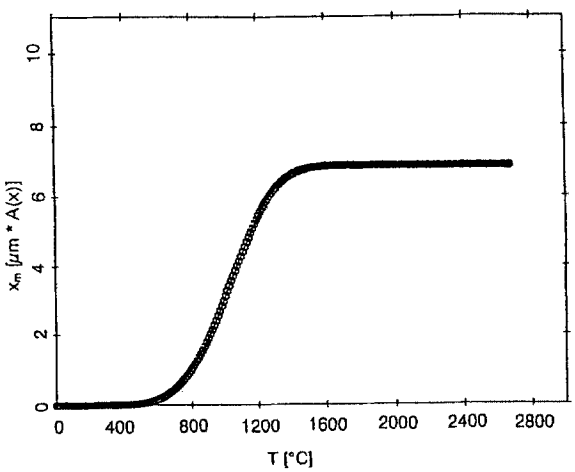

Fig. 6 Plot of the equation used for fitting the difference curves of the non-isothermal series measured during the high temperature corrosion of nickel

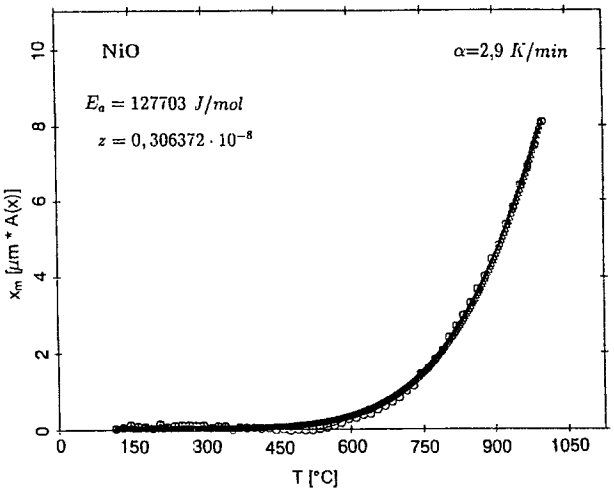

Fig. 7 Observed and fitted difference curves of a non-isothermal series measured during the high temperature corrosion of nickel

Before fitting activation energy E_a, preexponential factor z and calibration factor f_c the experimental difference curve $Y(T_j)$ is normalized and multiplied with the approximate thickness of the layer. The obtained curve $x_m(T)$ represents the thickness of the layer before correcting for the absorption, which facilitates the choice of the starting value of f_c for the fit. Figure 7 shows the experimental and the fitted curve. When the activation energies E_a are obtained from short experiments, they are higher than the literature values usually obtained from experiments of more than 100 h. This indicates that the diffusion rates through the layer are different at the beginning and after longer measuring times. Micrographs show that at the beginning of the oxidation small NiO-grains are formed facilitating intergranular diffusion.

Evaluation by peak fitting

HMX is presented as an example, where fitting of the diffraction peaks with a Lorentz function was used for thermal analysis [25, 26]. The explosive substance is used in applications, where safety aspects play an important role. The substance crystallizes in 4 phases, α-, β-, γ- and the high temperature phase δ-HMX with a considerably increased mechanical sensitivity. For estimating potential hazards the phase transition into and from the high temperature phase had to be determined. Thermal analysis by means of X-ray diffraction was chosen for an unambiguous identification of the phases. Fitting of the peaks yields peak position, intensity and the peak width. In Fig. 8 the intensities of peaks of the phases occurring during a temperature cycle starting with β-HMX are plotted. The plots reveal that after the transition into δ, a reconversion didn't occur even on cooling below room temperature. Repeated measurements after cooling at room temperature proved that a re-

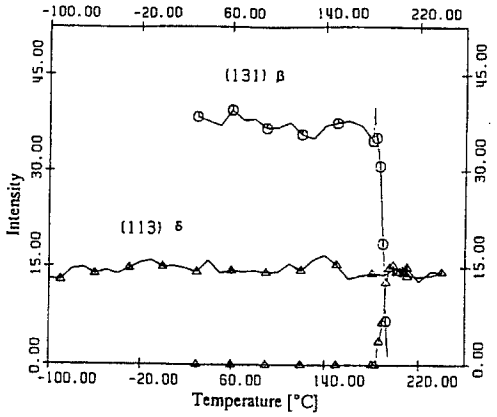

Fig. 8 Intensities of peaks of β- and δ-HMX measured during a temperature cycle

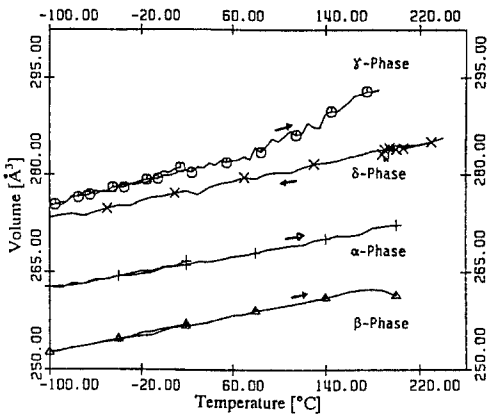

Fig. 9 Volumetric expansion curves of the HMX-phases calculated from diffraction patterns measured on heating and cooling

conversion can take days or even weeks, which requires careful treatment after unintentional heating.

The measured series can also be used for determining the thermal expansion of the phases by fitting the volume of the elementary phases from the peak positions, as can be seen in Fig. 9. Following the peak positions allowed also to detect an unusual behaviour of the γ -phase, which shows an irreversible change on heating before the transition into δ-HMX.

Evaluation with Rietveld refinement

Though the time consuming peak fitting can provide interesting results, Rietveld refinement has become the more powerful tool for extracting structural details from

powder diffraction data [5, 6]. The method applied to series of ammonium nitrate yielded the volumetric expansion curves in Fig. 10. Due to the uncomplete phase transitions during the temperature cycles the expansion curves of the phases could be determined beyond the thermodynamic phase limits. The curves reflect clearly the close relationship of the phases V and II and the smooth transition.

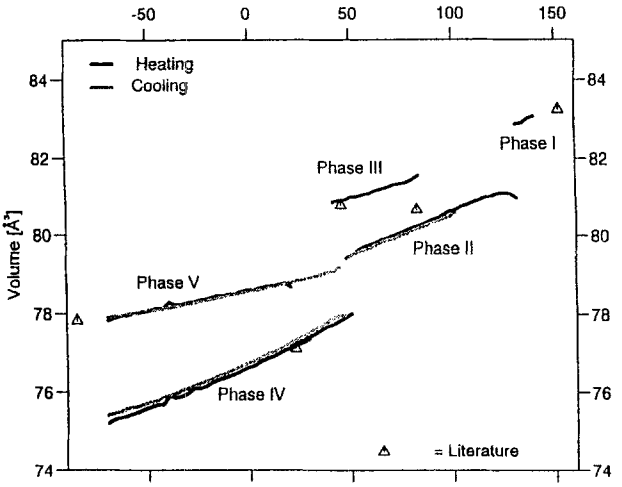

Fig. 10 Volumetric expansion curves of ammonium nitrate phases calculated from diffraction patterns of a temperature cycle by means of Rietveld refinement

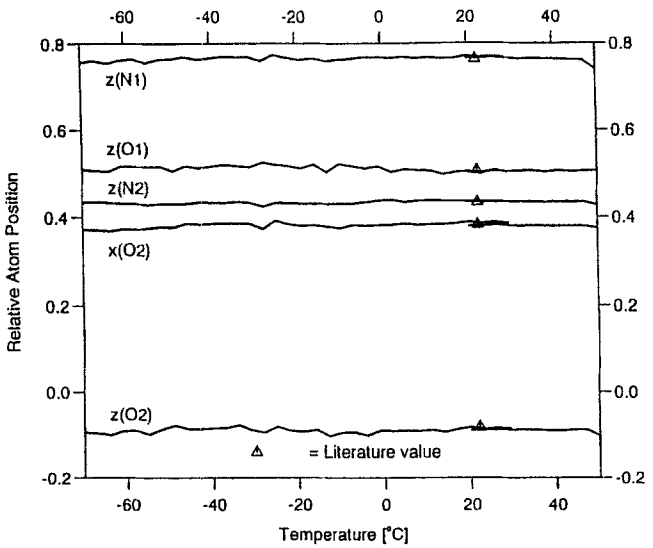

Fig. 11 Relative atom positions in the elementary cell of ammonium nitrate phase IV calculated from diffraction patterns of a temperature cycle by means of Rietveld refinement

Beside the volumetric curves the linear expansion coefficients i.e. the trace of the elementary cell parameters against temperature are available with the same data, which give a good picture of the anisotropy of the expansion especially with phase IV allowing interesting conclusions on the lattice dynamics.

Still more detailed informations are revealed by plotting the fitted atom positions against temperature. In Fig. 11 the constant atom positions relative to the expanding elementary cell mean that the nitrate groups in phase IV behave more or less as rigid bodies.

Conclusions and further development

The examples were given to demonstrate, how thermal analysis by means of time and temperature resolved X-ray diffraction can provide detailed structural informations on crystalline materials surpassing and complementing the possibilities of the classical tools like DSC and TG.

The future looks bright for the technique, as new X-ray optics will bring more intensities to the samples [27]. Especially the focusing optics will renew the interest for Debye-Scherrer geometries. The sample position in small capillaries will facilitate the construction of simultaneous diffraction pattern and DSC recording.

Optical devices delivering higher intensities together with new detectors will shorten the measuring times so that heating rates closer to the conventional techniques will become possible, though the possibilites of the synchrotron facilities with measurements down to the sub second range cannot be reached.

The evaluation by Rietveld refinement will be elaborated for dealing with extended series, thereby reducing the time requirements [28].

* * *

We are indebted to Mr. K. O. Hartmann, Mr. H. Fietzek and Mr. H. G. Farr for their assistance during the measurements and for the maintenance of the measuring systems.

References

1 B. B. Giessen and G. E. Gordon, Science, 159 (1968) 973.
2 S. K. Byram, R.A. Sparks et al., Advances in X-ray Analysis, 20 (1977) 529.
3 N. Eisenreich and W. Engel, J. Thermal Anal., 35 (1989) 577.
4 N. Eisenreich and W. Engel, J. Appl. Cryst., 16 (1983) 259.
5 H. M. Rietveld, Acta Cryst., 22 (1967) 151.
6 R. A. Young and D. B. Wiles, J. Appl. Cryst., 15 (1982) 430.
7 S. B. Hendricks, E. Posnjak and F. C. Kracek, J. Amer. Chem. Soc., 54 (1932) 2766.
8 N. L. Bowen, J. Phys. Chem., 30 (1926) 721.
9 M. Ahtee and K. J. Smolander, Acta Cryst., B39 (1983) 685.
10 C. S. Choi and J. E. Mapes, Acta Cryst., B28 (1972) 1357.
11 B. W. Lucas, Acta Cryst., B36 (1980) 2005.
12 B. W. Lucas, Acta Cryst., B35 (1979) 1038.
13 M. Ahtee and K. Kurki-Suonio, Acta Cryst., A35 (1979) 591.
14 K. Heide, Z. Anorg. Chem., 344 (1966) 241.
15 E. J. Griffith, J. Chem. Eng. Data, 8 (1963) 22.
16 R. N. Brown and A. C. McLaren, Proc. Royal Soc., 266A (1962) 329.

17 R. R. Sowell, M. M.Karnowsky and L. C. Walters, J. Thermal Anal., 3 (1971) 119.
18 J. S. Ingman, G. J. Kearley and S. F. A. Kettle, J. Chem. Soc., Far. Trans, 78 (1982) 1817.
19 V. Kolarik, Diplomarbeit 1989, Fraunhoferinstitut f. Chem. Techn., D76327 Berghausen.
20 S. Mathew and N. Eisenreich, W. Engel, Thermochim. Acta, 269/270 (1995) 475.
21 M. Avrami, J. Chem. Phys., 7 (1939) 1103.
22 B. V. Erofe'ev, C. R. Dokl. Acad. Sci. URSS, (1946) 511.
23 W. Jander, Z. Anorg. Allgem. Chem., 163 (1927) 1.
24 V. Kolarik, Thesis 1993, Fraunhoferinstitut f. Chem. Techn., D76327 Berghausen.
25 M. J. Herrmann, W. Engel and N. Eisenreich, Z. f. Krist., 204 (1993) 121.
26 M. J. Herrmann, W. Engel and N. Eisenreich, Prop., Expl., Pyrotechn., 17 (1992) 190.
27 M. Schuster and H. Gőbel, Applied Physics, 28 (1995) 270.
28 M. J. Herrmann et al., Materials Science Forum, Proc. of the Europ. Powder Diff. Conf. (EPDIC4), in print.